

**Precise measurement of the branching fractions for
 $B_s^0 \rightarrow D_s^{(*)+} D_s^{(*)-}$ and first measurement of the $D_s^{*+} D_s^{*-}$
polarization using e^+e^- collisions**

S. Esen,³ A. J. Schwartz,³ H. Aihara,⁴⁶ D. M. Asner,³⁶ T. Aushev,¹² A. M. Bakich,⁴¹
K. Belous,¹¹ B. Bhuyan,⁷ A. Bozek,³¹ M. Bračko,^{22,13} T. E. Browder,⁵ V. Chekelian,²³
A. Chen,²⁸ P. Chen,³⁰ B. G. Cheon,⁴ K. Chilikin,¹² R. Chistov,¹² I.-S. Cho,⁵²
K. Cho,¹⁶ Y. Choi,⁴⁰ J. Dalseno,^{23,43} M. Danilov,¹² Z. Doležal,² A. Drutskoy,¹²
S. Eidelman,¹ M. Feindt,¹⁵ V. Gaur,⁴² J. Haba,⁶ T. Hara,⁶ H. Hayashii,²⁷ Y. Horii,²⁶
Y. Hoshi,⁴⁴ W.-S. Hou,³⁰ Y. B. Hsiung,³⁰ H. J. Hyun,¹⁸ T. Iijima,^{26,25} A. Ishikawa,⁴⁵
R. Itoh,⁶ M. Iwabuchi,⁵² Y. Iwasaki,⁶ T. Iwashita,²⁷ T. Julius,²⁴ J. H. Kang,⁵²
T. Kawasaki,³³ C. Kiesling,²³ H. O. Kim,¹⁸ K. T. Kim,¹⁷ M. J. Kim,¹⁸ Y. J. Kim,¹⁶
K. Kinoshita,³ B. R. Ko,¹⁷ S. Koblitz,²³ P. Kodyš,² S. Korpar,^{22,13} R. T. Kouzes,³⁶
P. Križan,^{20,13} P. Krokovny,¹ T. Kuhr,¹⁵ T. Kumita,⁴⁸ Y.-J. Kwon,⁵² S.-H. Lee,¹⁷
J. Li,³⁹ Y. Li,⁵⁰ J. Libby,⁸ C. Liu,³⁸ Y. Liu,³ D. Liventsev,¹² R. Louvot,¹⁹ S. McOnie,⁴¹
H. Miyata,³³ R. Mizuk,¹² D. Mohapatra,³⁶ A. Moll,^{23,43} N. Muramatsu,³⁷
M. Nakao,⁶ H. Nakazawa,²⁸ Z. Natkaniec,³¹ C. Ng,⁴⁶ S. Nishida,⁶ K. Nishimura,⁵
O. Nitoh,⁴⁹ T. Ohshima,²⁵ S. Okuno,¹⁴ S. L. Olsen,^{39,5} Y. Onuki,⁴⁶ G. Pakhlova,¹²
C. W. Park,⁴⁰ H. Park,¹⁸ H. K. Park,¹⁸ T. K. Pedlar,²¹ R. Pestotnik,¹³ M. Petrič,¹³
L. E. Piilonen,⁵⁰ M. Röhrken,¹⁵ S. Ryu,³⁹ Y. Sakai,⁶ D. Santel,³ L. Santelj,¹³
T. Sanuki,⁴⁵ Y. Sato,⁴⁵ O. Schneider,¹⁹ C. Schwanda,¹⁰ K. Senyo,⁵¹ M. E. Sevier,²⁴
M. Shapkin,¹¹ T.-A. Shibata,⁴⁷ J.-G. Shiu,³⁰ B. Shwartz,¹ A. Sibidanov,⁴¹ F. Simon,^{23,43}
P. Smerkol,¹³ Y.-S. Sohn,⁵² A. Sokolov,¹¹ E. Solovieva,¹² S. Stanič,³⁴ M. Starič,¹³
T. Sumiyoshi,⁴⁸ G. Tatishvili,³⁶ Y. Teramoto,³⁵ K. Trabelsi,⁶ T. Tsuboyama,⁶
M. Uchida,⁴⁷ S. Uehara,⁶ T. Uglov,¹² Y. Unno,⁴ S. Uno,⁶ S. E. Vahsen,⁵ P. Vanhoefer,²³
G. Varner,⁵ C. H. Wang,²⁹ M.-Z. Wang,³⁰ P. Wang,⁹ Y. Watanabe,¹⁴ K. M. Williams,⁵⁰
E. Won,¹⁷ J. Yamaoka,⁵ Y. Yamashita,³² Z. P. Zhang,³⁸ V. Zhilich,¹ and V. Zhulanov¹

(The Belle Collaboration)

- ¹*Budker Institute of Nuclear Physics SB RAS and
Novosibirsk State University, Novosibirsk 630090*
- ²*Faculty of Mathematics and Physics, Charles University, Prague*
- ³*University of Cincinnati, Cincinnati, Ohio 45221*
- ⁴*Hanyang University, Seoul*
- ⁵*University of Hawaii, Honolulu, Hawaii 96822*
- ⁶*High Energy Accelerator Research Organization (KEK), Tsukuba*
- ⁷*Indian Institute of Technology Guwahati, Guwahati*
- ⁸*Indian Institute of Technology Madras, Madras*
- ⁹*Institute of High Energy Physics, Chinese Academy of Sciences, Beijing*
- ¹⁰*Institute of High Energy Physics, Vienna*
- ¹¹*Institute of High Energy Physics, Protvino*
- ¹²*Institute for Theoretical and Experimental Physics, Moscow*
- ¹³*J. Stefan Institute, Ljubljana*
- ¹⁴*Kanagawa University, Yokohama*
- ¹⁵*Institut für Experimentelle Kernphysik,
Karlsruher Institut für Technologie, Karlsruhe*
- ¹⁶*Korea Institute of Science and Technology Information, Daejeon*
- ¹⁷*Korea University, Seoul*
- ¹⁸*Kyungpook National University, Taegu*
- ¹⁹*École Polytechnique Fédérale de Lausanne (EPFL), Lausanne*
- ²⁰*Faculty of Mathematics and Physics, University of Ljubljana, Ljubljana*
- ²¹*Luther College, Decorah, Iowa 52101*
- ²²*University of Maribor, Maribor*
- ²³*Max-Planck-Institut für Physik, München*
- ²⁴*University of Melbourne, School of Physics, Victoria 3010*
- ²⁵*Graduate School of Science, Nagoya University, Nagoya*
- ²⁶*Kobayashi-Maskawa Institute, Nagoya University, Nagoya*
- ²⁷*Nara Women's University, Nara*
- ²⁸*National Central University, Chung-li*
- ²⁹*National United University, Miao Li*
- ³⁰*Department of Physics, National Taiwan University, Taipei*

- ³¹*H. Niewodniczanski Institute of Nuclear Physics, Krakow*
- ³²*Nippon Dental University, Niigata*
- ³³*Niigata University, Niigata*
- ³⁴*University of Nova Gorica, Nova Gorica*
- ³⁵*Osaka City University, Osaka*
- ³⁶*Pacific Northwest National Laboratory, Richland, Washington 99352*
- ³⁷*Research Center for Electron Photon Science, Tohoku University, Sendai*
- ³⁸*University of Science and Technology of China, Hefei*
- ³⁹*Seoul National University, Seoul*
- ⁴⁰*Sungkyunkwan University, Suwon*
- ⁴¹*School of Physics, University of Sydney, NSW 2006*
- ⁴²*Tata Institute of Fundamental Research, Mumbai*
- ⁴³*Excellence Cluster Universe, Technische Universität München, Garching*
- ⁴⁴*Tohoku Gakuin University, Tagajo*
- ⁴⁵*Tohoku University, Sendai*
- ⁴⁶*Department of Physics, University of Tokyo, Tokyo*
- ⁴⁷*Tokyo Institute of Technology, Tokyo*
- ⁴⁸*Tokyo Metropolitan University, Tokyo*
- ⁴⁹*Tokyo University of Agriculture and Technology, Tokyo*
- ⁵⁰*CNP, Virginia Polytechnic Institute and State University, Blacksburg, Virginia 24061*
- ⁵¹*Yamagata University, Yamagata*
- ⁵²*Yonsei University, Seoul*

Abstract

We have made a precise measurement of the absolute branching fractions of $B_s^0 \rightarrow D_s^{(*)+} D_s^{(*)-}$ decays using 121.4 fb^{-1} of data recorded by the Belle experiment running at the $\Upsilon(5S)$ resonance. The results are $\mathcal{B}(B_s^0 \rightarrow D_s^+ D_s^-) = (0.58_{-0.09}^{+0.11} \pm 0.13)\%$, $\mathcal{B}(B_s^0 \rightarrow D_s^{*\pm} D_s^{\mp}) = (1.76_{-0.22}^{+0.23} \pm 0.40)\%$, and $\mathcal{B}(B_s^0 \rightarrow D_s^{*+} D_s^{*-}) = (1.98_{-0.31}^{+0.33} \text{ }_{-0.50}^{+0.52})\%$; the sum is $\mathcal{B}(B_s^0 \rightarrow D_s^{(*)+} D_s^{(*)-}) = (4.32_{-0.39}^{+0.42} \text{ }_{-1.03}^{+1.04})\%$. Assuming $B_s^0 \rightarrow D_s^{(*)+} D_s^{(*)-}$ saturates decays to CP -even final states, the branching fraction constrains the ratio $\Delta\Gamma_s / \cos\phi_{12}$, where $\Delta\Gamma_s$ is the difference in widths between the two B_s - \bar{B}_s mass eigenstates, and ϕ_{12} is the CP -violating phase in B_s - \bar{B}_s mixing. We also measure for the first time the longitudinal polarization fraction of $B_s^0 \rightarrow D_s^{*+} D_s^{*-}$; the result is $0.06_{-0.17}^{+0.18} \pm 0.03$.

Decays of B_s mesons help elucidate the weak Cabibbo-Kobayashi-Maskawa structure of the Standard Model (SM). B_s decays can be studied at e^+e^- colliders by running at the $\Upsilon(5S)$ resonance, which decays to $B_s^{(*)}\bar{B}_s^{(*)}$ pairs. We have used this method previously [1] to study $B_s^0 \rightarrow D_s^{(*)+}D_s^{(*)-}$ decays using 23.6 fb^{-1} of data. Here we substantially improve this measurement using 121.4 fb^{-1} of data. In addition to the five-times-larger data set, there are other improvements to the analysis: the data have been fully reprocessed using reconstruction algorithms with higher efficiency for π^0 's and low momentum tracks; we use larger control samples to evaluate systematic uncertainties; and we take background probability density functions directly from data rather than from simulation. We also make the first measurement of the fraction of longitudinal polarization (f_L) of $B_s^0 \rightarrow D_s^{*+}D_s^{*-}$.

As in our previous study, we reconstruct the final states $D_s^+D_s^-$, $D_s^{*+}D_s^- + D_s^{*-}D_s^+$ ($\equiv D_s^{\pm}D_s^{\mp}$), and $D_s^{*+}D_s^{*-}$. These are expected to be mostly CP -even, and their partial widths are expected to dominate the difference in widths between the two B_s - \bar{B}_s CP eigenstates, $\Delta\Gamma_s^{CP}$ [2]. This parameter equals $\Delta\Gamma_s/\cos\phi_{12}$, where $\Delta\Gamma_s$ is the decay width difference between the mass eigenstates, and $\phi_{12} = \arg(-M_{12}/\Gamma_{12})$, where M_{12} and Γ_{12} are the off-diagonal elements of the B_s - \bar{B}_s mass and decay matrices [3]. The phase ϕ_{12} is the CP -violating phase in B_s - \bar{B}_s mixing. Thus the branching fraction gives a constraint in the $\Delta\Gamma_s$ - ϕ_{12} parameter space. Both parameters can receive contributions from new physics (NP) [4, 5]. Previous constraints on $\Delta\Gamma_s$ and NP contributions to ϕ_{12} were obtained from a time-dependent angular analysis of $B_s \rightarrow J/\psi \phi$ decays [6–8]. A constraint on ϕ_{12} can be derived from the CP asymmetry measured in B_s semileptonic decays [9].

At the $\Upsilon(5S)$ resonance, the $e^+e^- \rightarrow b\bar{b}$ cross section is measured to be $\sigma_{b\bar{b}} = 0.340 \pm 0.016 \text{ nb}$, and the fraction of $\Upsilon(5S)$ decays producing B_s mesons is $f_s = 0.172 \pm 0.030$ [10]. Thus the total number of $B_s\bar{B}_s$ pairs is $N_{B_s\bar{B}_s} = (121.4 \text{ fb}^{-1}) \cdot \sigma_{b\bar{b}} \cdot f_s = (7.11 \pm 1.30) \times 10^6$. Three production modes are kinematically allowed: $B_s\bar{B}_s$, $B_s\bar{B}_s^*$ or $B_s^*\bar{B}_s$, and $B_s^*\bar{B}_s^*$. The production fractions ($f_{B_s^{(*)}\bar{B}_s^{(*)}}$) for the latter two are 0.073 ± 0.014 and 0.870 ± 0.017 , respectively [11]. The B_s^* decays via $B_s^* \rightarrow B_s\gamma$, and the γ is not reconstructed.

The Belle detector running at the KEKB e^+e^- collider [12] is described in Ref. [13]. For charged hadron identification, a likelihood ratio is formed based on dE/dx measured in the central tracker and the response of aerogel threshold Čerenkov counters and time-of-flight scintillation counters. A likelihood requirement is used to identify charged kaons and pions. This requirement is 86% efficient for K^\pm and has a π^\pm misidentification rate of 8%.

We reconstruct $B_s^0 \rightarrow D_s^+ D_s^-$, $D_s^{*\pm} D_s^\mp$, and $D_s^{*+} D_s^{*-}$ decays in which $D_s^+ \rightarrow \phi \pi^+$, $K_S^0 K^+$, $\bar{K}^{*0} K^+$, $\phi \rho^+$, $K_S^0 K^{*+}$, and $\bar{K}^{*0} K^{*+}$ [14]. Neutral K_S^0 candidates are reconstructed from $\pi^+ \pi^-$ pairs having an invariant mass within 10 MeV/ c^2 of the nominal K_S^0 mass [15] and satisfying momentum-dependent vertex requirements. Charged tracks are required to originate from near the $e^+ e^-$ interaction region and, with the exception of tracks from K_S^0 decays, have a momentum $p > 100$ MeV/ c . Neutral K^{*0} (charged K^{*+}) candidates are reconstructed from a $K^+ \pi^-$ ($K_S^0 \pi^+$) pair having an invariant mass within 50 MeV/ c^2 of m_{K^*} . Candidate ϕ mesons are reconstructed from $K^+ K^-$ pairs having an invariant mass within 12 MeV/ c^2 of m_ϕ . Charged ρ^+ candidates are reconstructed from $\pi^+ \pi^0$ pairs having an invariant mass within 100 MeV/ c^2 of m_{ρ^+} . The π^0 candidates are reconstructed from $\gamma \gamma$ pairs having an invariant mass within 15 MeV/ c^2 of m_{π^0} , and with each γ having an energy $E_\gamma > 100$ MeV.

The invariant mass windows used for the reconstructed D_s^+ candidate (denoted \widetilde{D}_s^+) are: ± 10 MeV/ c^2 ($\sim 3\sigma$) for the three final states containing K^* candidates, ± 20 MeV/ c^2 (2.8σ) for $\phi \rho^+$, and ± 15 MeV/ c^2 ($\sim 4\sigma$) for the remaining two modes. For the three vector-pseudoscalar final states we require $|\cos \theta_{\text{hel}}| > 0.20$, where θ_{hel} is the angle between the momentum of the charged daughter of the vector particle and the direction opposite the \widetilde{D}_s^+ momentum, evaluated in the rest frame of the vector particle.

We combine D_s^+ candidates with photon candidates to reconstruct $D_s^{*+} \rightarrow D_s^+ \gamma$ decays. We require $E_\gamma > 50$ MeV in the $e^+ e^-$ center-of-mass system, and that the energy deposited in the central 3×3 array of cells of the electromagnetic cluster exceeds 85% of that deposited in the central 5×5 array of cells. The mass difference $M_{\widetilde{D}_s^+ \gamma} - M_{\widetilde{D}_s^+}$ is required to be within 12.0 MeV/ c^2 of the nominal value. This requirement and also that of the \widetilde{D}_s^+ mass windows are determined by optimizing a figure-of-merit $S/\sqrt{S+B}$, where S is the expected signal based on Monte Carlo (MC) simulation and B is the background estimated from either MC simulation or D_s^+ mass sideband data.

We select $B_s^0 \rightarrow D_s^+ D_s^-$, $D_s^{*\pm} D_s^\mp$, and $D_s^{*+} D_s^{*-}$ decays using two quantities evaluated in the center-of-mass frame: the beam-energy-constrained mass $M_{\text{bc}} = \sqrt{E_{\text{beam}}^2 - p_B^2}$, and the energy difference $\Delta E = E_B - E_{\text{beam}}$, where p_B and E_B are the reconstructed momentum and energy of the B_s^0 candidate, and E_{beam} is the beam energy. We determine signal yields by fitting events satisfying $5.25 \text{ GeV}/c^2 < M_{\text{bc}} < 5.45 \text{ GeV}/c^2$ and $-0.15 \text{ GeV} < \Delta E < 0.10 \text{ GeV}$. Because the γ from $B_s^* \rightarrow B_s \gamma$ is not reconstructed, the modes $\Upsilon(5S) \rightarrow B_s \bar{B}_s$, $B_s \bar{B}_s^*$ and $B_s^* \bar{B}_s^*$ are well-separated in M_{bc} and ΔE . We expect only small contributions

from $B_s\bar{B}_s$ and $B_s\bar{B}_s^*$ events and fix these contributions relative to $B_s^*\bar{B}_s^*$ according to our measurement using $B_s^0 \rightarrow D_s^-\pi^+$ decays [11]. We quote fitted signal yields from $B_s^*\bar{B}_s^*$ only and use these to determine the branching fractions.

Approximately half of selected events have multiple $B_s^0 \rightarrow D_s^{(*)+}D_s^{(*)-}$ candidates. These typically arise from photons produced via $\pi^0 \rightarrow \gamma\gamma$ that are wrongly assigned as D_s^* daughters. For these events we select the candidate that minimizes the quantity

$$\frac{1}{(2+N)} \left\{ \sum_{D_s} \left[\frac{M_{\tilde{D}_s} - M_{D_s}}{\sigma_M} \right]^2 + \sum_{D_s^*} \left[\frac{\Delta\tilde{M} - \Delta M}{\sigma_{\Delta M}} \right]^2 \right\},$$

where $\Delta\tilde{M} = M_{\tilde{D}_s^+\gamma} - M_{\tilde{D}_s^+}$ and $\Delta M = M_{D_s^{*+}} - M_{D_s^+}$. The summations run over the two D_s^+ daughters and the N ($=0, 1, 2$) D_s^{*+} daughters of a B_s^0 candidate. The mean masses $M_{D_s^{(*)}}$ and widths σ_M and $\sigma_{\Delta M}$ are obtained from MC simulation and calibrated for data-MC differences using a large $B^0 \rightarrow D_s^{(*)+}D^-$ control sample from $\Upsilon(4S)$ data. According to the simulation, this criterion selects the correct candidate 83%, 73%, and 69% of the time for $D_s^+D_s^-$, $D_s^{*\pm}D_s^\mp$, and $D_s^{*+}D_s^{*-}$ states, respectively.

We reject background from $e^+e^- \rightarrow q\bar{q}$ ($q = u, d, s, c$) events using a Fisher discriminant based on a set of modified Fox-Wolfram moments [16]. This discriminant distinguishes jet-like $q\bar{q}$ events from more spherical $B_{(s)}\bar{B}_{(s)}$ events. With this discriminant we calculate likelihoods \mathcal{L}_s and $\mathcal{L}_{q\bar{q}}$ for an event assuming the event is signal or $q\bar{q}$ background; we then require $\mathcal{L}_s/(\mathcal{L}_s + \mathcal{L}_{q\bar{q}}) > 0.20$. This selection is 93% efficient for signal events and removes more than 62% of $q\bar{q}$ background events.

The remaining background consists of $\Upsilon(5S) \rightarrow B_s^{(*)}\bar{B}_s^{(*)} \rightarrow D_s^+X$, $\Upsilon(5S) \rightarrow B\bar{B}X$ ($b\bar{b}$ hadronizes to B^0 , \bar{B}^0 , or B^\pm), and $B_s \rightarrow D_{s,J}^\pm(2317)D_s^{(*)}$, $D_{s,J}^\pm(2460)D_s^{(*)}$, or $D_s^\pm D_s^\mp \pi^0$. The last three processes peak at negative ΔE , and their yields are estimated to be small using analogous $B_d \rightarrow D_{s,J}^\pm D^{(*)}$ branching fractions. We thus consider them only when evaluating systematic uncertainty due to backgrounds. All selection criteria are finalized before looking at events in the signal region.

We measure signal yields by performing a two-dimensional unbinned maximum-likelihood fit to the $M_{bc}-\Delta E$ distributions. For each sample, we include probability density functions (PDFs) for signal and $q\bar{q}$, $B_s^{(*)}\bar{B}_s^{(*)} \rightarrow D_s^+X$, and $\Upsilon(5S) \rightarrow BBX$ backgrounds. As the backgrounds have similar M_{bc} and ΔE shapes, we use a single PDF for them, taken to be an ARGUS function [17] for M_{bc} and a first-order Chebyshev function for ΔE . The two

parameters of the Chebyshev function are taken from data in which one of the D_s^+ candidates is required to be within the mass sideband.

The signal PDFs have three components: correctly reconstructed (CR) decays; “wrong combination” (WC) decays in which a non-signal track or γ is included in place of a true daughter track or γ ; and “cross-feed” (CF) decays in which a $D_s^{*\pm}D_s^\mp$ ($D_s^{*+}D_s^{*-}$) is reconstructed as a $D_s^+D_s^-$ ($D_s^+D_s^-$ or $D_s^{*\pm}D_s^\mp$), or a $D_s^+D_s^-$ ($D_s^{*\pm}D_s^\mp$) is reconstructed as a $D_s^{*\pm}D_s^\mp$ or $D_s^{*+}D_s^{*-}$ ($D_s^{*+}D_s^{*-}$). In the former case, the γ from $D_s^{*+} \rightarrow D_s^+\gamma$ is lost and ΔE is shifted down by 100–150 MeV; this is called “CF-down.” In the latter case, an extraneous γ is included and ΔE is shifted up by a similar amount; this is called “CF-up.” In both cases M_{bc} remains almost unchanged.

All signal shape parameters are taken from MC simulation and calibrated using $B_s^0 \rightarrow D_s^{(*)-}\pi^+$ and $B^0 \rightarrow D_s^{(*)+}D^-$ decays. The CR PDF is taken to be a Gaussian for M_{bc} and a double Gaussian with common mean for ΔE . The CF and WC PDFs consist of sums of Gaussians and a Chebyshev function for ΔE , and Gaussians and either a Novosibirsk function [18] or a Crystal Ball function [19] for M_{bc} . The fractions of WC and CF-down events are taken from the simulation. The fractions of CF-up events are floated as they are difficult to simulate accurately (i.e., many B_s^0 partial widths are unmeasured). As the CF-down fractions are fixed, the separate $D_s^+D_s^-$, $D_s^{*\pm}D_s^\mp$, and $D_s^{*+}D_s^{*-}$ samples are fitted simultaneously.

The projections of the fit are shown in Fig. 1, and the fitted signal yields are listed in Table I. The branching fraction for channel i is calculated as $\mathcal{B}_i = Y_i/(\varepsilon_{MC}^i \cdot N_{B_s\bar{B}_s} \cdot f_{B_s^*\bar{B}_s^*} \cdot 2)$, where Y_i is the fitted CR yield, and ε_{MC}^i is the MC signal efficiency with intermediate branching fractions [15] included. The efficiencies ε_{MC}^i include small correction factors to account for differences between MC and data for kaon identification. Inserting all values gives the branching fractions listed in Table I. These results have similar precision as other recent measurements [20] and are in agreement with theoretical predictions [21, 22]. The statistical significance is calculated as $\sqrt{-2 \ln(\mathcal{L}_0/\mathcal{L}_{\max})}$, where \mathcal{L}_0 and \mathcal{L}_{\max} are the values of the likelihood function when the signal yield Y_i is fixed to zero and when it is floated, respectively. We include systematic uncertainties (discussed below) in the significance by smearing the likelihood function by a Gaussian having a width equal to the total systematic error related to the signal yield.

The systematic errors are listed in Table II. The error due to PDF shapes is evaluated by

varying shape parameters by $\pm 1\sigma$. The errors for the fixed WC and CF-down fractions are evaluated by repeating the fit with each fixed fraction varied by $\pm 20\%$. Those fractions that are correlated (e.g., WC for $D_s^* D_s^+$ and $D_s^{*+} D_s^{*-}$, which is due to reconstructing extraneous photons) are varied together in the ratio predicted from MC simulation. The systematic errors due to $q\bar{q}$ suppression and the best candidate selection are evaluated using control samples of $B_s^0 \rightarrow D_s^- \pi^+$ and $B^0 \rightarrow D_s^{(*)+} D^-$, respectively. These errors are taken as the change in the branching fractions when the criteria are applied. The uncertainties due to π^\pm/K^\pm identification and tracking efficiency are obtained from $D^{*+} \rightarrow D^0 \pi^+ \rightarrow K^- \pi^+ \pi^+$ decays; these are $\sim 1\%$ and 0.35% per track, respectively. Significant uncertainties arise from the $\Upsilon(5S) \rightarrow B_s^* \bar{B}_s^*$ and D_s^+ branching fractions, which are external factors. We take the $D_s^{*+} D_s^{*-}$ polarization f_L for this measurement to be the well-measured value from the analogous decay $B_d^0 \rightarrow D_s^{*+} D^{*-}$: 0.52 ± 0.05 [15]. The systematic error is taken as the change in \mathcal{B} when f_L is varied over a wide range: from 2σ higher than 0.52 down to the (low) central value we measure below.

TABLE I: $B_s^* \bar{B}_s^*$ CR signal yield (Y) and efficiency (ε), including intermediate branching fractions, and resulting branching fraction (\mathcal{B}) and signal significance (S), including systematic errors. The first errors listed are statistical; the others are systematic. The last error for the sum is due to external factors ($\Upsilon(5S) \rightarrow B_s^* \bar{B}_s^*$ and D_s^+ branching fractions).

Mode	Y (events)	ε ($\times 10^{-4}$)	\mathcal{B} (%)	S
$D_s^+ D_s^-$	$33.1^{+6.0}_{-5.4}$	4.72	$0.58^{+0.11}_{-0.09} \pm 0.13$	11.5
$D_s^{*\pm} D_s^\mp$	$44.5^{+5.8}_{-5.5}$	2.08	$1.76^{+0.23}_{-0.22} \pm 0.40$	10.1
$D_s^* D_s^*$	$24.4^{+4.1}_{-3.8}$	1.01	$1.98^{+0.33}_{-0.31} {}^{+0.52}_{-0.50}$	7.8
Sum	$102.0^{+9.3}_{-8.6}$		$4.32^{+0.42}_{-0.39} {}^{+0.56}_{-0.54} \pm 0.88$	

In the limits $m_{(b,c)} \rightarrow \infty$ with $(m_b - 2m_c) \rightarrow 0$ and N_c (number of colors) $\rightarrow \infty$, the $D_s^{*\pm} D_s^\mp$ and $D_s^{*+} D_s^{*-}$ modes are CP -even and (along with $D_s^+ D_s^-$) saturate the width difference $\Delta\Gamma_s^{CP}$ [2]. Assuming negligible CP violation ($\phi_{12} \approx 0$), the branching fraction is related to $\Delta\Gamma_s$ via $\Delta\Gamma_s/\Gamma_s = 2\mathcal{B}/(1 - \mathcal{B})$. Inserting the total \mathcal{B} from Table I gives $\Delta\Gamma_s/\Gamma_s =$

TABLE II: Systematic errors (%). Those listed in the top section affect the signal yield and thus the signal significance.

Source	$D_s^+ D_s^-$		$D_s^* D_s$		$D_s^{*+} D_s^{*-}$	
	$+\sigma$	$-\sigma$	$+\sigma$	$-\sigma$	$+\sigma$	$-\sigma$
Signal PDF shape	2.7	2.2	2.2	2.4	5.1	3.8
Bckgrnd PDF shape	1.5	1.3	1.3	1.4	2.9	2.8
WC + CF fraction	0.5	0.5	4.7	4.5	11.0	9.7
$q\bar{q}$ suppression	3.1	0.0	0.0	2.7	0.0	2.1
Best cand. selection	5.5	0.0	1.5	0.0	1.5	0.0
π^\pm/K^\pm identif.	7.0	7.0	7.0	7.0	7.0	7.0
K_S reconstruction	1.1	1.1	1.1	1.1	1.1	1.1
π^0 reconstruction	1.1	1.1	1.1	1.1	1.1	1.1
γ	-	-	3.8	3.8	7.6	7.6
Tracking	2.2	2.2	2.2	2.2	2.2	2.2
Polarization	0.0	0.0	0.8	2.8	0.6	0.2
MC statistics for ε	0.2	0.2	0.4	0.4	0.5	0.5
$D_s^{(*)}$ br. fractions	8.6	8.6	8.6	8.6	8.7	8.7
$N_{B_s^{(*)} B_s^{(*)}}$			18.3			
$f_{B_s^* \bar{B}_s^*}$			2.0			
Total	22.7	21.8	22.7	22.9	26.2	25.5

$0.090 \pm 0.009 \pm 0.023$, where the first error is statistical and the second is systematic. The central value is consistent with, but lower than, the theoretical prediction [4]; the difference may be due to the unknown CP -odd component in $B_s^0 \rightarrow D_s^{*+} D_s^{*-}$, and contributions from three-body final states. With more data these unknowns can be measured. The former is estimated to be only 6% for analogous $B^0 \rightarrow D^{*+} D_s^{*-}$ decays [23], but the latter can be significant: Ref. [22] calculates $\Delta\Gamma(B_s \rightarrow D_s^{(*)} D^{(*)} K^{(*)})/\Gamma_s = 0.064 \pm 0.047$. This calculation predicts $\Delta\Gamma_s/\Gamma_s$ from $D_s^{(*)+} D_s^{(*)-}$ alone to be 0.102 ± 0.030 , which agrees well with our result. This agreement holds for ϕ_{12} values up to $\sim 40^\circ$ [24].

To measure f_L , we select events using the same criteria as before but, to minimize $B_s^0 \rightarrow D_s^{*\pm} D_s^\mp$ cross-feed, we use a narrower range of M_{bc} and ΔE (2.5σ in resolution). For these events we perform an unbinned ML fit to the helicity angles θ_1 and

θ_2 , which are the angles between the daughter γ momentum and the opposite of the B_s momentum in the D_s^{*+} and D_s^{*-} rest frames, respectively. The angular distribution is $(|A_+|^2 + |A_-|^2)(\cos^2 \theta_1 + 1)(\cos^2 \theta_2 + 1) + |A_0|^2 4 \sin^2 \theta_1 \sin^2 \theta_2$, where A_+ , A_- , and A_0 are the three polarization amplitudes in the helicity basis. The fraction f_L equals $|A_0|^2/(|A_0|^2 + |A_+|^2 + |A_-|^2)$. To account for resolution and efficiency variation, the signal PDFs are taken from MC. The background PDF is taken from an M_{bc} sideband; the level (1.8 ± 0.7 events) is estimated from a D_s^+ mass sideband and fixed in the fit. We obtain

$$f_L = 0.06_{-0.17}^{+0.18} \pm 0.03, \quad (1)$$

where the systematic errors arise from: signal PDF shapes ($+0.008, -0.010$), the background PDF shape ($+0.007, -0.004$), fixed WC fractions ($+0.013, -0.015$), the fixed background level (± 0.022), $q\bar{q}$ suppression ($+0.011, -0$), possible fit bias ($+0, -0.011$), and MC efficiency due to statistics (± 0.0004). The helicity angle distributions and fit projections are shown in Fig. 2.

In summary, we have measured the branching fractions for $B_s^0 \rightarrow D_s^{(*)+} D_s^{(*)-}$ using e^+e^- data taken at the $\Upsilon(5S)$ resonance. Under some theoretical assumptions and neglecting CP violation, the total branching fraction gives a constraint on $\Delta\Gamma_s/\Gamma_s$. We have also made the first measurement of the $B_s^0 \rightarrow D_s^{*+} D_s^{*-}$ longitudinal polarization fraction.

We thank R. Aleksan and L. Oliver for useful discussions. We thank the KEKB group for excellent operation of the accelerator; the KEK cryogenics group for efficient solenoid operations; and the KEK computer group, the NII, and PNNL/EMSL for valuable computing and SINET4 network support. We acknowledge support from MEXT, JSPS and Nagoya's TL-PRC (Japan); ARC and DIISR (Australia); NSFC (China); MSMT (Czechia); DST (India); INFN (Italy); MEST, NRF, GSDC of KISTI, and WCU (Korea); MNiSW (Poland); MES and RFAAE (Russia); ARRS (Slovenia); SNSF (Switzerland); NSC and MOE (Taiwan); and DOE and NSF (USA).

-
- [1] S. Esen *et al.* (Belle Collab.), Phys. Rev. Lett. **105**, 201802 (2010).
 - [2] R. Aleksan *et al.*, Phys. Lett. B **316**, 567 (1993).
 - [3] I. Dunietz, R. Fleischer, and U. Nierste, Phys. Rev. D **63**, 114015 (2001); I. Dunietz, Phys. Rev. D **52**, 3048 (1995).

- [4] A. Lenz and U. Nierste, arXiv:1102.4274; Jour. High Energy Phys. **0706**, 072 (2007).
- [5] See for example: A.J.Buras *et al.*, JHEP **1010**, 009 (2010); Z. Ligeti *et al.*, Phys. Rev. Lett. **105**, 131601 (2010).
- [6] V. M. Abazov *et al.* (DØ Collab.), Phys. Rev. D **85**, 032006 (2012).
- [7] T. Aaltonen *et al.* (CDF Collab.), Phys. Rev. D **85**, 072002 (2012).
- [8] R. Aaij *et al.* (LHCb Collab.), Phys. Rev. Lett. **108**, 101803 (2012).
- [9] Y. Amhis *et al.* (Heavy Flavor Averaging Group), arXiv:1207.1158 (2012).
- [10] These results are obtained by Belle using 121.4 fb^{-1} of data and the method described in A. Drutskoy *et al.* (Belle Collab.), Phys. Rev. Lett. **98**, 052001 (2007).
- [11] This result is obtained by Belle using 121.4 fb^{-1} of data and the method described in R. Louvot *et al.* (Belle Collab.), Phys. Rev. Lett. **102**, 021801 (2009).
- [12] S. Kurokawa and E. Kikutani, Nucl. Instrum. and Methods Phys. Res. A **499**, 1 (2003), and other papers included in this volume.
- [13] A. Abashian *et al.* (Belle Collab.), Nucl. Instr. Meth. Phys. Res. A **479**, 117 (2002).
- [14] Charge-conjugate modes are implicitly included.
- [15] K. Nakamura *et al.* (Particle Data Group), J. Phys. G **37**, 075021 (2010), and 2011 update.
- [16] G. C. Fox and S. Wolfram, Phys. Rev. Lett. **41**, 1581 (1978). The modified moments used in this paper are described in S. H. Lee *et al.* (Belle Collab.), Phys. Rev. Lett. **91**, 261801 (2003).
- [17] H. Albrecht *et al.* (ARGUS Collab.), Phys. Lett. B **241**, 278 (1990).
- [18] The Novosibirsk function is defined as $f(x) = A \exp(-0.5\{\ln^2[1 + \Lambda\tau \cdot (x - x_0)]/\tau^2 + \tau^2\})$, where $\Lambda = \sinh(\tau\sqrt{\ln 4})/(\sigma\tau\sqrt{\ln 4})$.
- [19] T. Skwarnicki, Ph.D. thesis, Institute for Nuclear Physics, Krakow 1986; DESY F31-86-02 (1986).
- [20] T. Aaltonen *et al.* (CDF Collab.), Phys. Rev. Lett. **108**, 201801 (2012).
- [21] R.-H. Li, C.-D. Lu, A. I. Sanda, and X.-X. Wang, Phys. Rev. D **81**, 034006 (2010).
- [22] C.-K. Chua, W.-S. Hou, and C.-H. Shen, Phys. Rev. D **84**, 074037 (2011).
- [23] J. Rosner, Phys. Rev. D **42**, 3732 (1990).
- [24] For $\phi_{12} \neq 0$ the relationship becomes $\Delta\Gamma_s/\Gamma_s = (1 - \sqrt{1 - 4\mathcal{B}(1 - \mathcal{B}) \cos^2 \phi_{12}})/[(1 - \mathcal{B}) \cos \phi_{12}]$, where \mathcal{B} includes all CP -even decay modes.

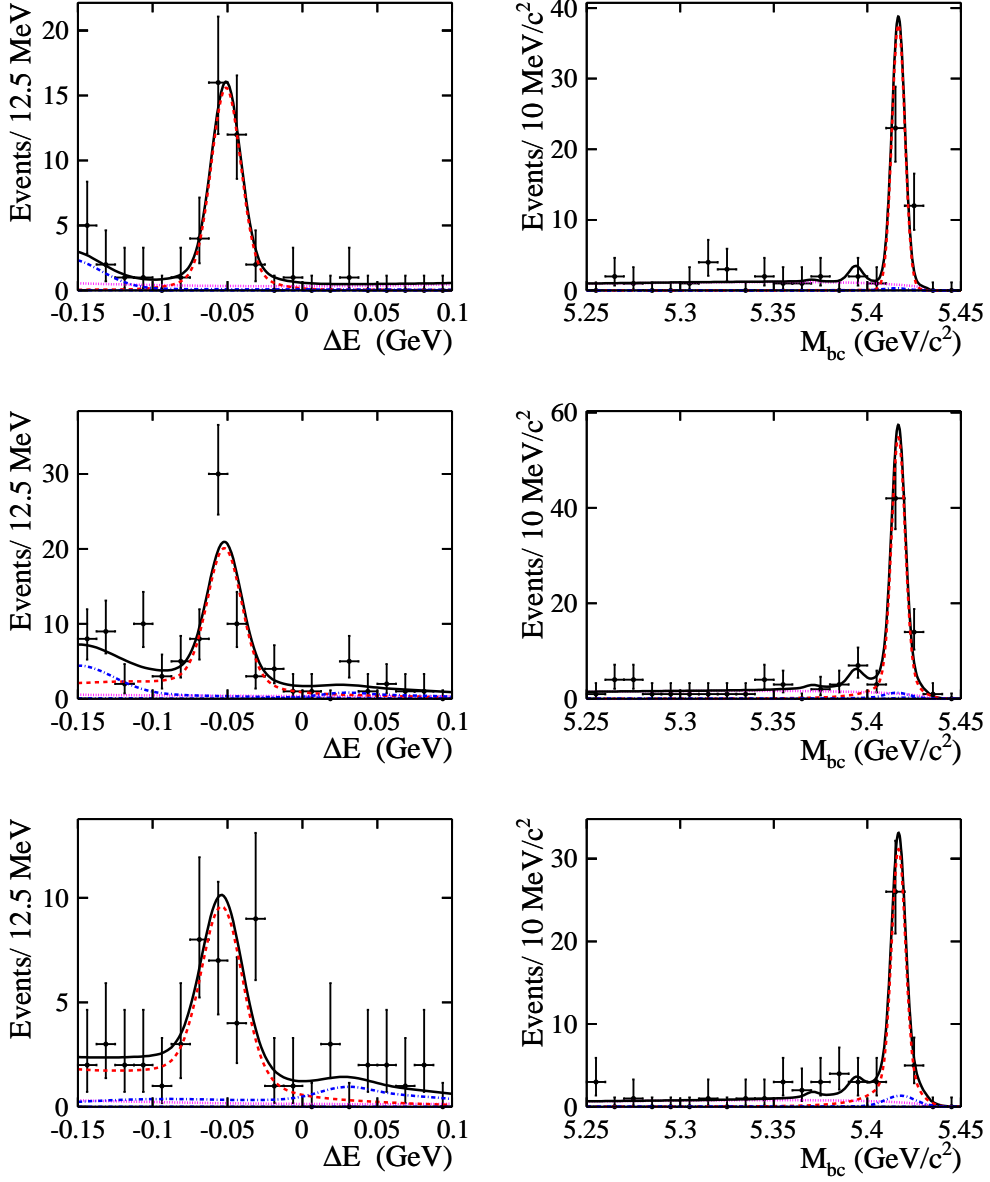


FIG. 1: ΔE fit projections for events satisfying $M_{bc} \in [5.41, 5.43] \text{ GeV}/c^2$, and M_{bc} fit projections for events satisfying $\Delta E \in [-0.08, -0.02] \text{ GeV}$. The top row shows $B_s^0 \rightarrow D_s^+ D_s^-$; the middle row shows $B_s^0 \rightarrow D_s^{*\pm} D_s^{\mp}$; and the bottom row shows $B_s^0 \rightarrow D_s^{*+} D_s^{*-}$. The red dashed curves show CR+WC signal; the blue dash-dotted curves show CF; the magenta dotted curves show background; and the black solid curves show the total.

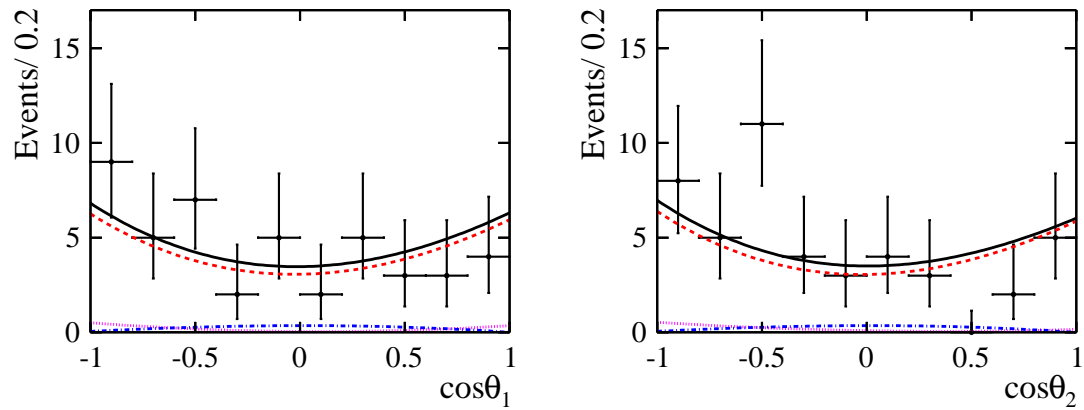


FIG. 2: Helicity angle distributions and projections of the fit result. The red dashed (blue dash-dotted) curves show the transverse (longitudinal) components; the magenta dotted curves show background; and the black solid curves show the total.